International Journal of Science and Research (IJSR)
ISSN (Online): 2319-7064
Index Copernicus Value (2013): 6.14 | Impact Factor (2015): 6.391

Synthesis, Characterization and Ammonia Sensing Properties of Mn Doped Zinc Oxide Nano-Composite

Saroj D. Patil[1], R. B. Waghulade[2], R. S. Khadayate[3]

[1]GF's – Godavari College of Engineering, Jalgaon 425001, Maharashtra, India

[2]D.N.C.V.P's Arts, Commerce and Science College, Jalgaon 425001, Maharashtra, India

[3]G.D.M. Arts, K.R.N. Commerce, M.D. Science College, Jamner, Dist-Jalgaon, Maharashtra, India

Abstract: ***This paper reports the synthesis, characterization and ammonia sensing properties of nano-sized Zinc oxide (ZnO) and its nano composite Mn doped ZnO. A simple chemical co-precipitation method is used for the synthesis of ZnO nano-sized powder and its nano-composite. Zinc Acetate ($Zn(C_2H_3O_2)_2$) , Manganese acetate ($Mn(CH_3COO)_2 \cdot 2H_2O$) and the sodium hydroxide (NaOH) were used as a starting materials and double distilled water as a carrier. The resulting nano-sized powder was characterized by x-ray diffraction (XRD) measurements, transmission electron microscopy (TEM) and energy dispersive x-ray (EDAX). The NH_3 sensing properties of the synthesized nano-sized ZnO were investigated at different operating temperatures and NH_3 concentrations. The effects of operating temperature on the sensitivity, selectivity, response and recovery of the sensor in the presence of NH_3 and other gases were studied and discussed.***

Keywords: Nano-sized Mn doped ZnO, Chemical co-precipitation, XRD, TEM, EDAX, NH_3 gas sensor

1. Introduction

Over the past few years, the synthesis and functionalism of nanostructures have attracted great interest due to their significant potential application. Recently, semiconductor nanostructures have attracted much interest due to their extraordinary physical properties and potentials for diverse electronic and photonic device applications [1,2].

Zinc oxide (ZnO), one of the very important and versatile semiconductors with direct band gap of gap of 3.37 eV [3] and a large exciton binding energy of 60 meV [4] at room temperature (RT) is a promising candidate for functional components of devices and materials in photonic crystals [5], gas sensors [6], light emitting diodes [7], solar cells [8, 9], lasers [2], varistors [10] and photoelectrochemical cells [11]. Over the past few years, ZnO nanomaterials with various interesting structures and properties have been synthesized, such as nanoparticles [12], nanorods [13], nanobelts, nanocombs [14], nanowires [15], and tetrapod nanostructures [16]. It is well known that doping a selective element into ZnO is the primary method for controlling the properties of the semiconductor such as band gap or electrical conductivity, and to increase the carrier concentration for electronic applications where a higher carrier concentration is required. Recently, many studies have focused on the doping of transition metals (TMs) such as Mn, Ni, Fe, Co and Cr into ZnO due to the potential applications in spintronics [17].

Ammonia is used in many chemical industries, fertilizer factories, refrigeration systems, food processing, medical diagnosis, fire power plants etc. A leak in the system can result the health hazards. Ammonia is harmful and toxic [18-22] in nature. Detection of low concentration of ammonia is not only important from the points discussed above but also, it is very important from the view of chemical pollution in the production of silicon devices in clean rooms. It is therefore necessary to monitor ammonia gas and to develop the ammonia gas sensors. Efforts are made to develop the ZnO -based gas sensors, which should detect ammonia at low temperature.

Few room temperature ammonia sensors are already available [23, 24], but having comparatively low response. Despite of high sensitivity, selectivity and long-term stability, the main drawback of such sensors is that they are operated at high temperature (>300°C). Also, the noble metal additives like Pt, Pd, Au, and Ag to a base material like ZnO, for the modification, increases the cost of the sensors. Therefore the applicability of these sensors remains limited. Hence the sensors operable at room temperature with low cost metal additives must be developed for large applicability.

2. Experimental

2.1 Preparation of nano-powder

Undoped and Mn-doped zinc oxide nanocrystals have been synthesized in aqueous solutions by using zinc acetate (Zn $(CH_3COO)_2$, $2H_2O$), manganese acetate ($Mn(CH_3COO)_2$, $2H_2O$) and sodium hydroxide (NaOH) as the starting materials. Aqueous solution of zinc acetate and manganese acetate at room temperature was stirred using a magnetic stirrer. Then the NaOH solution was added slowly drop wise to aqueous solution of zinc acetate and manganese acetate under constant stirring until the final solution pH value of about 8 was achieved. The resulting precipitate was filtered and washed three to four times using double distilled water to remove impurities. The hydroxide, thus formed was dried at 100^0C and grinded into a powder, which is the precursor.

The precursor was calcined in air at different temperatures of 400^0C, 600^0C, 800^0C and 1000^0C for 2 hours to produce nano-crystalline powders with different grain size.

2.2 Preparation of Pallet

The nano powder was be pressed into pallete having thickness 0.120cm under pressure of 5 tons using the Pelletizer machine and the ohmic contacts were done with the silver paste to form the sensing elements.

2.3 Characterisation

The structure of the calcined powder was investigated by using X-ray diffraction (XRD) technique. The X-ray diffraction patterns were recorded with a Rigaku diffractometer (Miniflex Model, Rigaku, Japan) having Cu K_α (λ = 0.1542 nm). The crystalline size was estimated from the broadening of Mn-ZnO (101) diffraction peak (2θ = 36.31^0C) using Debye-Scherrer's formula. The transmission electron microscopy (TEM) was used to determine the particle size and the morphology of the nano-sized powder with JEOL 1200 EX. The composition of elements like Zn, O and Mn is confirmed by energy dispersive x-ray (EDAX) spectra.

2.4 Details of the gas sensing system

The gas sensing was carried out on these sensing elements with laboratory design static gas chamber to sense different gases in air atmosphere. The sensing element was placed directly on the metal plate. The temperature of the metal plate was varied with the help of heater and the temperature was measured with the help of aluminium-chromel thermocouple. The known volume of the sensing gas was introduced into the gas chamber. The electrical resistance of the sensing element was measured before and after exposer to gas using sensitive digital multimeter (METRAVI 603)

3. Materials Characterisations

3.1 Structural Properties (X-ray Diffraction)

The XRD pattern of the calcinied powder at 400^0C for 2 hour is shown in Fig. 1.

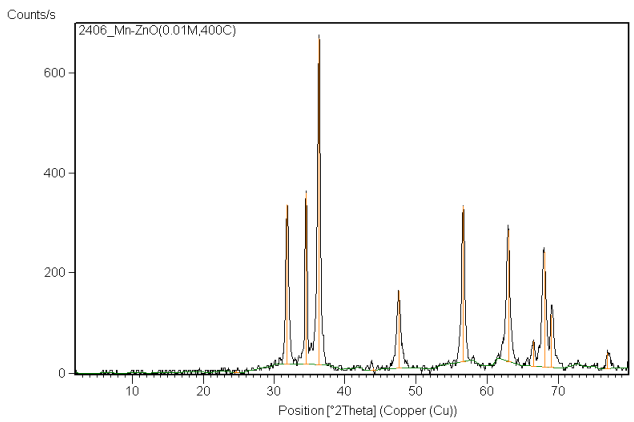

Figure 1: XRD pattern of Mn doped ZnO calcinied at 400^0C

The XRD indicates the major diffraction peaks at 2θ values of 31.80^0, 34.46^0, 36.31^0, 47.58^0, 56.67^0, 63.01^0, 68.98^0, and 76.95^0 etc which are attributed to the formation of Mn - ZnO. The peak positions are agree well with cassiterite structure. From the XRD data it is clear that, there are no peaks corresponding to Mn^{2+} ions. This indicates that there is no alteration of wurtzite structure of ZnO due to substitution of Mn^{2+} ions. The crystallite size was calculated by using the Scherrer formula –

$$t = \frac{k\lambda}{B\cos\theta}$$

where t is the average size of the crystallite, assuming that the grains are spherical, k is 0.9, λ is the wavelength of X-ray radiation, B is the peak full width at half maximum (FWHM) and θ is the angle of diffraction. The crystalline size of the powder calcinied at 400^0C is found to be minimum and it is ~35.31 nm scale.

3.2 TEM Micrograph

The TEM micrograph of the powder calcinied at 400^0C is shown in Fig. 2. The TEM micrograph shows clearly that the particle size of powder calcinied at 400^0C is in nm scale. This result is in well agreement with the crystallite size calculated using the XRD data.

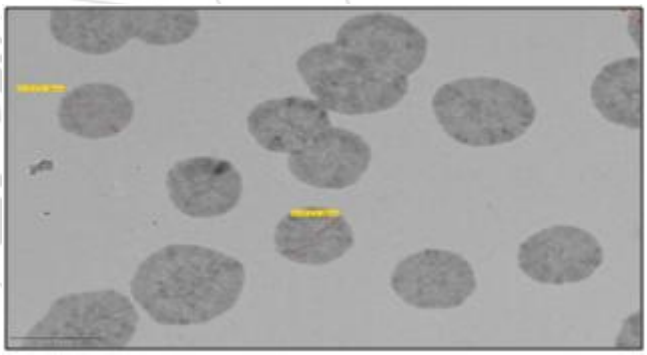

Figure 2: TEM micrograph of Mn doped ZnO calcinied at 400^0C for 2h

3.3 Quantitative elemental analysis

The EDAX spectram of nano-sized Mn-ZnO is as shown in Fig. 3. The EDAX analysis indicates the presence of signals due to the Zn (33.95%), Mn (5.43%), and O (60.62%), which proves that the formation of the nanocomposote without any impurities.

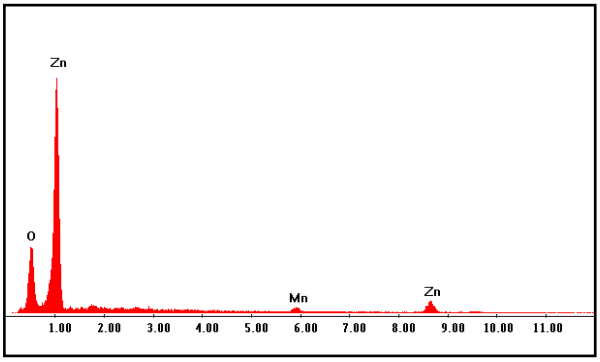

Figure 3: EDAX spectram of Mn doped ZnO

4. Gas sensing performance of the sensor

4.1 Sensing performance of pure ZnO

The gas response of the sensing element is defined as:

$$S(\%) = \frac{R_g - R_a}{R_a} \; x \; 100$$

where R_a and R_g are the resistance values of the sensor element in air and in the presence gaseous environment.

Fig 4 shows the variation of gas response with operating temperature of pure ZnO to 2500 ppm of ammonia gas. The gas response increases with increase in operating temperature and it is maximum at 400^0C. For pure ZnO gas response is 19.64 % at 400^0C to NH_3. The NH_3 gas response of pure ZnO is related to oxygen adsorption on surface. The oxygen adsorption is poor for pure ZnO and shows poor response to NH_3. ZnO requires more temperature to adsorb oxygen ions. Hence it would have higher response at higher operating temperature [26].

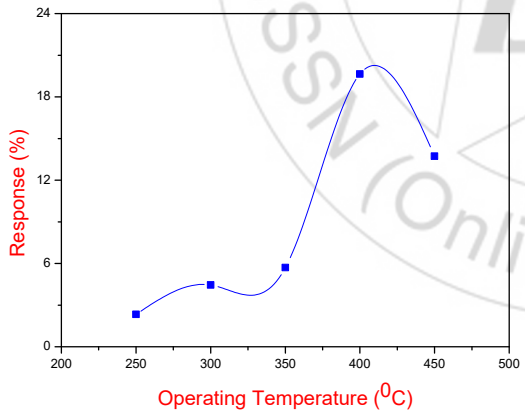

Figure 4: Effect of operating temperature on gas response of pure Nano ZnO

4.2 Sensing performance of Mn doped ZnO

A. Effect of operating temperature

Fig 5 shows the effect of operating temperature on gas response to NH_3 gas (2500 ppm) for Mn doped ZnO. Mn doped ZnO shows maximum response 50.82 % to 90^0C. At this temperature there would be no adsorption, hence the oxygen adsorption-desorption is not employed to sense the NH_3 gas. When raising the temperature above 90^0C, the moisture from the surface evaporates and hence the response would decreases [27].

In comparision of Pure ZnO there is increased sensing response of the Mn-doped ZnO. This is might be due to the decreased crystallite size and enhanced electron density [28]. This may also be due to the excess donor concentrations induced by Mn doping [29,30]. Since Mn^{2+} has lower ionization energy than that of ZnO, it might have influenced the oxygen adsorption / desorption process [31]. Hence Mn doped ZnO showed an excellent response than undoped ZnO film.

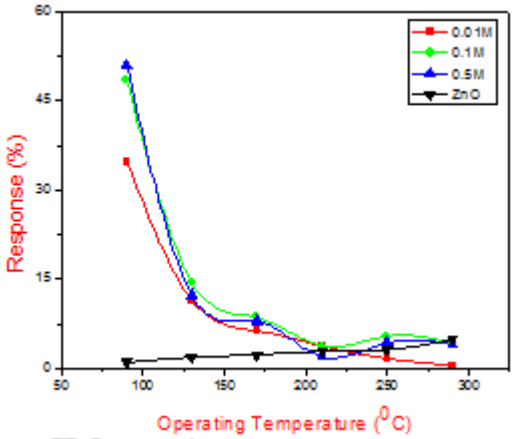

Figure 5: Effect of operating temperature on gas response of Mn doped ZnO

B. Effect of gas concentration

Fig 6 shows the effect of NH_3 gas concentration at 90^0C to Mn doped ZnO. This sensor was exposed to varying concentrations of NH_3 it shows continuously increase in gas response with increase in concentrations. This is due to, the low gas concentration gives a lower surface coverage of gas molecules which results into lower surface reaction between the adsorbed oxygen species at surface and the gas molecules. The increase in the gas concentration increases the surface reaction due to a large surface coverage [32].

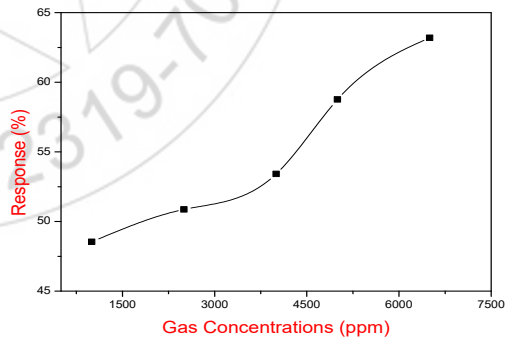

Figure 6: Dependance of sensitivit on NH_3 gas concentration at operating temperating 90^0C

C. Selectivity of NH_3 gas

Selectivity or specificity is defined as the ability of a sensor to respond to certain gas in the presence of other different gases. Fig 7 shows the selectivity of Mn doped ZnO for NH_3 sensor. Sensor shows maximum selectivity among the various gases like LPG, Methanol, acetone and H_2S at 90^0C.

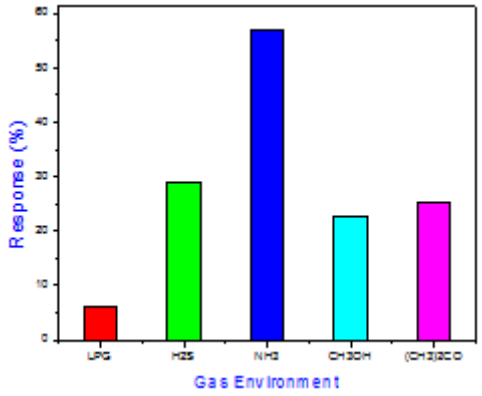

Figure 7: Selectivity curve of Mn doped ZnO to2500 ppm to various gases

D. Response and recovery time

Response time is defined as the time required to reach 90% of the maximum increase in response when the gas is turned on. And recovery time is defined as the time required to get back 90% of the maximum response in air. Fig 8 shows the quick response (10 Sec.) and fast recovery (50 Sec.) to NH3 gas.

When ammonia is exposed, due to surface reaction of ammonia with physisorbed H_2O or by conductivity through NH_4^+ cations, resistance gets decreases. It constitutes the proton conductivity leading to decrease in resistance. This would decrease the barrier height among the MnO_2-ZnO.

$$NH_3 + H_2O \longrightarrow NH_4OH$$

During the surface reaction, produced NH_4OH is volatile in nature. This high volatile nature explains the quick response and fast recovery time of the sensor [25].

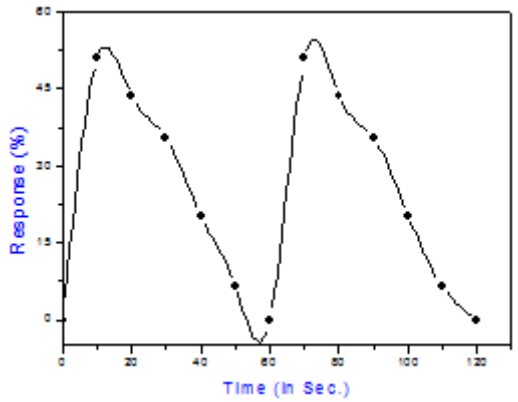

Figure 8: Response and recovery of sensor for NH_3 gas

5. Conclusions

The following main findings resulted from the present investigation –

- We have successfully synthesized the Mn doped ZnO nano-composite at low cost by using a chemical co-precipitation method . Zinc Acetate ($\mathbf{Zn(C_2H_3O_2)_2}$) , mangnese acetate ($\mathbf{Mn(CH_3COO)_2 \cdot 2H_2O}$) and the sodium hydroxide (NaOH) were used as a starting materials and double distilled water as a carrier. The resulting powder was characterized by XRD measurements, TEM and EDAX.
- The crystallite size is found to be 35. 31 nm when the as-prepared powder was calcinied at 400°C for 2 h.
- The operating temperature significantly affects the sensitivity of the synthesized Mn doped ZnO nano-composite to the NH_3. The sensitivity to 2500 ppm of NH_3 is maximum at an operating temperature 90°C and it was found to be ~ 50.82 %. The response time was nearly 10 s and the recovery time was found to be 50 s.
- It was shown that Mn doped ZnO nano-composite can be reliably used to monitor the concentration of NH_3 over the range (1000-6500 ppm).

References

[1] X. Duan, Y. Huang, Y. Cui, J.Wang and C.M. Lieber: Nature, 2001, 409, 66.
[2] H.M. Huang, S. Mao, H. Feick, H. Yan, H. Wu and H. Kind: Science, 2001, 292, 1897.
[3] Meyer B K et al 2004 Physica Status Solidi B 241 231
[4] Madelung O (ed) 1992 Data in Science and Technology: Semiconductors (Berlin: Springer)
[5] Chen Y, Bagnall D and Yao T 2000 Mater. Sci. Eng. B 75 190
[6] Dayan N J, Sainkar S R, Karekar R N and Aiyer R C 1998 Thin Solid Films 325 254
[7] Saito N, Haneda H, Sekiguchi T, Ohashi N, Sakaguchi L and Koumoto K 2002 Adv. Mater. 14 418
[8] Chopra K L and Das S R 1983 Thin Film Solar Cells (New York: Plenum) 321
[9] Salam S, Islam M, Alam M, Akram A, Ikram M, Mahmood A, Khan M and Mujahid M 2011 Adv. Nature Sci.: Nanosci. Nanotechnol. 2 045001
[10] Hung N T, Quang N D and Bernik S 2001 Mater. Res. 16 2817
[11] Chieng D T, Long P D, Lam N H and Hoi P V 2010 Adv. Nature Sci.: Nanosci. Nanotechnol. 1 035010
[12] Dong L F, Cui L Z and Zhang Z K 1997 Nanostruct. Mater. 8 815
[13] Wu J J and Liu S C 2002 Adv. Mater. 14 215
[14] Yang P D, Yan H Q, Mao S, Russo R, Johnso J, Saykally R, Morris N, Pham J R, He R and Choj H J 2002 Adv. Funct.Mater. 12 323
[15] Kong Y C, Yu D P, Zhang B, Fang W and Feng S Q 2001 Appl. Phys. Lett. 78 407
[16] Dai Y, Zhang Y, Li Q K and Nan C W 2002 Chem. Phys. Lett. 83 358
[17] Bauer C, Boschloo G, Mukhtar E and Hagfeldt A 2001 J.Phys. Chem. B 105 5585
[18] L. R. Narasimhan, W. Goodman, C. Kumar and N. Patel, Proceedings of the National Academy of Sciences, Vol. 98, No. 8, 2001, pp. 4617-4621. doi:10.1073/pnas.071057598
[19] R. E. de la Hoz, D. P. Schueter and W. N. Rom, American Journal of Indus-trial Medicine, Vol. 29, 1996, pp. 209-214. doi:10.1002/(SICI)1097-0274(199602)29:2<209::AID-AJIM12>3.0.CO;2-7
[20] C. M. Leung and C. L. Foo, Annals Academy of Medicine Singapore, Vol. 21, 1992, pp. 624-629.

doi:10.1289/ehp.99107617
[21] 21 R. A. Michaels, Environmental Health Perspectives, Vol. 107, No. 8, 1999, pp. 617-627.
[22] L. G. Close, F. I. Catlin and A. M. Cohn, Archives of Otolaryngology, Vol. 106, No. 3, 1980, pp. 151-158.
[23] S.Durgajanani, B.G. Jeyaprakash, R.J. Bosco Balaguru, Influence of precursor concentration on structural, morphological and electrical properties of spray deposited ZnO thin films, Cryst. Res. Technol. 46 (2011) 685-690
[24] P.Singh, A. Kaushal, D. Kaur, Mn-doped ZnO nanocrystalline trhin films prepared by ultrasonic spray pyrolysis, J. Alloy Compd. 471 (2009) 11-15
[25] S. Senthilkumar, K. Rajendran, S. Banerjee, T.K. Chini, V. Sengodan, Influence of Mn doping on the microstructure and optical property of ZnO, Mater. Sci. Semicond. Process, 11 (2008) 6-12
[26] D. R. Patil, L. A. Patil and P. P. Patil, Sensors and Actuators B, Vol. 126, 2007, pp. 368-374. doi:10.1016/j.snb.2007.03.028
[27] G. S. Trivikrama Rao and D. Tarakarama Rao, Sensors and Actuators B, Vol. 55, 1999, pp. 166-169. doi:10.1016/S0925-4005(99)00049-0
[28] L. A. Patil, L. S. Sonawane and D. G. Patil Journal of Modern Physics,2011, 2, 1215-1221,doi:10.4236/jmp.2011210150
[29] X. Peng, J. Chu, B. Yang, P. X. Feng, Sens. Actuat. B 174 (2012) 258.
[30] D. Sivalingam, J. B. Gopalakrishnan, J. B. B. Rayappan, Sens. Actuat. B 166-167 (2012) 624.
[31] X. Peng, J. Chu, B. Yang, P. X. Feng, Sens. Actuat. B 174 (2012) 258.
[32] Y. Mao, S. Ma, X. Li, C. Wang, F. Li, X. Yang, J. Zhu, L. Ma, Appl. Surf. Sci. 298 (2014) 109.